Design and development of a computer-assisted retinal laser surgery system

Cameron H. G. Wright
Steven F. Barrett
University of Wyoming
Laramie, Wyoming 82071

Ashley J. Welch
University of Texas at Austin
Austin, Texas 78712

Abstract. Since the mid-1980s, the development of a therapeutic, computer-assisted laser photocoagulation system to treat retinal disorders has progressed under the guidance of Dr. Welch, the Marion E. Forsman Centennial Professor of Engineering, Department of Biomedical Engineering, the University of Texas at Austin. This paper reviews the development of the system, related research in eye movement and laser-tissue interaction, and system implementation and testing. While subsets of these topics have been reported in prior publications, this paper brings the entire evolutionary design of the system together. We also discuss other recent "spinoff" uses of the system technology that have not been reported elsewhere and describe the impact of the latest technical advances on the overall system design.
[DOI: 10.1117/1.2342465]

Keywords: digital imaging; tracking; lasers in medicine; ophthalmology; optical engineering; biomedical optics.

Paper 05286SSR received Sep. 30, 2005; revised manuscript received Feb. 14, 2006; accepted for publication Feb. 14, 2006; published online Aug. 31, 2006.

1 Introduction

Laser photocoagulation has been used to treat retinal disorders such as diabetic retinopathy, macular degeneration, and retinal tears for several decades.[1] The laser's monochromatic, highly coherent beam is ideally suited for areas of the retina that are difficult or dangerous to reach using traditional invasive surgical techniques. A visible green (argon ion) laser is typically used for retinal treatment. The laser is directed through the patient's pupil and the intervening ocular media to the retina. The argon wavelength results in high absorption at the retinal pigment epithelium (RPE) underlying the neural retinal layers, which results in heat transfer to the neighboring tissue; a therapeutic lesion is thus formed. As the lesion forms it appears increasingly reflective compared to the surrounding tissue. The lesion reflects light more than the undamaged parts of the retina due to a heat-induced increase in the optical scattering coefficient of the tissue.[2,3]

Normal treatment protocols require placement of multiple therapeutic lesions on the retina.[4] Certain disorders, such as diabetic retinopathy, may require up to several thousand lesions per eye. Patients receive this treatment while fully alert in an outpatient environment, often over the course of multiple appointments. During the procedure, the patient's head is typically supported in a chin cup and the conjugate eye is stabilized via a fixation target. Even with this multimode stabilization technique, considerable retinal movement often occurs if the patient's attention on the fixation target drifts or if the patient blinks, sneezes, or otherwise moves.

Address all correspondence to Cameron Wright, Department of Electrical and Computer Engineering, University of Wyoming 1000 E. University Ave. - Dept 3295, Laramie, WY 82071; Tel: (307) 766-6104; Fax: (307) 766-2248 E-mail: c.h.g.wright@ieee.org

Traditional methods require each of the lesions to be placed manually. The ophthalmologist determines the appropriate lesion placement based on accepted treatment protocols and presets the laser for desired spot size, power, and irradiation time. A low power aiming laser is then directed to the desired therapeutic lesion location on the retina. The physician typically pauses to ascertain if the patient's fixation appears to be holding steady and, if so, engages the full therapeutic power of the laser by stepping on a foot pedal. The lesion is formed based on preset laser parameters using an average irradiation time of 100 ms. This process is repeated for each lesion one-by-one until the treatment is complete.

This manual lesion placement technique suffers from several drawbacks that have motivated the design and development of a computer-assisted system.[5,6] First, the treatment protocol is very tedious for both the patient and the ophthalmologist. Second, the laser pointing accuracy and safety margin are limited by a combination of the ophthalmologist's dexterity and the patient's ability to maintain visual stabilization. For example, only 20 ms of otherwise therapeutic laser energy deposited on the fovea due to retinal movement during irradiation can cause blindness.[4] Third, there is a large variability in lesion size even with identical irradiation parameters due to nonhomogeneous retinal tissue properties. The development of a computer-assisted laser delivery system would aid the ophthalmologist in therapeutic lesion placement and parameter control, increase patient safety, and improve the consistency of the laser-induced lesions. This paper reviews the development of such a system, related research in eye movement and laser-tissue interaction, and system implementation and testing.

1083-3668/2006/11(4)/041127/12/$22.00 © 2006 SPIE

2 Background

To give the reader a better understanding of the rationale in developing such a system, we provide a brief discussion of retinal eye diseases treatable with argon laser therapy and describe retinal eye movement.

2.1 *Retinal Pathologies Treatable With an Argon Laser*

Three common retinal diseases that are treatable with argon laser therapy are diabetic retinopathy, macular degeneration, and retinal tears.[7] We provide a brief description of each with an established treatment protocol using argon laser therapy. Keep in mind that all treatments are currently performed manually.

2.1.1 *Diabetic retinopathy*

Diabetic retinopathy is the most common of all retinal diseases and is one of the leading causes of blindness. It is a direct result of diabetes mellitus. In diabetic retinopathy, the retinal tissue senses that it lacks sufficient oxygen and responds by rapidly developing many new, typically low-quality, blood vessels in an effort to increase the retinal oxygen supply. Often these blood vessels leak, develop irregular branches, and obstruct the vision path to the fovea. This disease is treated by selectively placing small lesions (200 to 500 μm in diameter) in the peripheral portion of the retina while avoiding the healthy retinal blood vessel network and the area of acute vision (the fovea and the surrounding macular region). The lesion sites result in denatured tissue and reduce the overall oxygen demand by the retina and hence mitigate the retinopathy. This procedure may require up to 3000 lesions per eye.

2.1.2 *Macular degeneration*

Macular degeneration is most often associated with the older segment of the population and is the leading cause of blindness in the United States for people over 60 years old. In macular degeneration, the primary vision area of the retina (the macula) deteriorates, causing poor central vision. It is important to note that the fovea, the small spot in the center of the macula, is responsible for acute vision. For treatment, an argon laser is directed on the retina at different locations to stop leakage or bleeding associated with the disease. Lesion placement is extremely critical since treatment is often required near the fovea. As noted above, laser-induced damage to the fovea can cause permanent blindness.

2.1.3 *Retinal tears*

Retinal detachments are caused by disease or injury. The retinal layers become detached from the eye wall and usually result in the immediate loss (partial or complete) of vision in the detached area. Retinal detachment is often preceded by retinal tears. In a retinal tear, the vitreous fluid leaks into the torn area, creates pressure that pushes the neural layers away from the inner wall, and eventually separates and detaches the retinal layers. Thus if the tear can be repaired quickly, retinal detachment may be avoided. The procedure for laser treatment of retinal detachment or tears is to direct the argon laser to locations surrounding the damaged area and create a surrounding "fence" of lesions to stop the tears from progressing to a wider area of the eye or from precipitating a detachment.

2.1.4 *Other pathologies*

Aside from these more common retinal diseases, argon laser therapy has also been used to treat retinal vein occlusions, ocular histoplasmosis, central serous chorioretinopathy, and ocular tumors. Although these conditions are less common, they share similar treatment protocols with the previously described retinal disorders and involve a manually placed argon laser.

The key concern for the treatment of these disorders is the difficulty in placing therapeutic lesions due to their small size, short irradiation times, critical placement, and nonhomogeneous target tissue. Lesion placement is further complicated by eye movement. In Sec. 2.2, we will briefly review eye movement characteristics. Although fixation techniques are used to minimize eye movement during laser treatment, eye movement (and hence retinal movement) still occurs.

2.2 *Eye Movement*

Eye movement is controlled by external ocular muscles: the lateral rectus muscles for looking to the side, the medial rectus muscles for looking toward the nose, the superior rectus muscle for looking up, the inferior rectus muscle for looking down, and the superior and inferior oblique muscles for depressing and elevating the gaze. These muscles act in a coordinated fashion to move the eyes as a conjugate pair. The retinae, as relatively rigid ocular globes, also move in tandem with eye movement as a conjugate pair. The following is a brief review of eye movements listed from fastest to slowest.[8,9]

- Saccades are short duration (20 to 200 ms), rapid eye movements with velocities of up to 800 deg/s for visual target acquisition.
- Smooth pursuit and vergence movements are for tracking a slowly moving object to maintain the object's image on the foveae. Both of these systems are slow compared to the saccadic system but can accurately track up to approximately 50 deg/s.
- Optokinetic and vestibular-ocular movement systems are used to compensate for observer motion to maintain stable vision as a person moves.
- Microsaccades and micronystagmus movements are required to maintain visibility of stationary objects due to image fading. They occur approximately every second, shift the gaze by 5 to 10 min of arc, and are difficult to suppress.

In traditional manual photocoagulation procedures, eye fixation techniques are employed to minimize eye movements. However, it must be emphasized that eye movements still occur.[10] This makes the ophthalmologist's job more difficult and is a safety concern for the patient.

3 System Overview

To assist the physician in placing therapeutic lesions for retinal disorders, Welch initiated a research effort in the late 1980s to design, prototype, and test a clinically practical, computer-assisted system to:

- quickly and safely place therapeutic retinal lesions of desired parameters at desired retinal locations

- compensate for patient retinal movement
- compensate for variations in the retinal tissue properties
- provide consistent lesions across the face of the retina
- provide a user-friendly interface.

From these general goals, a list of specific system requirements was developed. The requirements included:

- retinal tracking rates equal to or better than 10 deg/s
- laser pointing accuracy better than 100 μm at the retinal surface
- uniform lesion formation within 5% of apparent size and depth
- system reaction time of no more than 5 ms
- ability to register a loss of tracking lock when a patient blinks or if the system is unable to keep up with the moving retina
- ability to automatically attempt to reestablish system lock when lost.

Many of Welch's graduate students worked on various aspects of this project. For the purposes of discussion, their efforts have been grouped according to the main subsystems to which they contributed: a digital eye tracking system, an analog eye tracking system, a retinal lesion parameter control system, and the overall user interface. When integrated together, these subsystems provide a hybrid system capable of mapping desired lesion placement sites, tracking and compensating for retinal movement, and controlling laser irradiation time to provide for consistent therapeutic lesions. In the following Secs. 3.1 to 3.3, we detail the development of each subsystem.

3.1 *Tracking System Development*

One of the key improvements to be provided by the computer-assisted system is to guard against undesirable and unanticipated eye movement during laser irradiation. If the eye moves during irradiation, the lesion site will not be where it was planned to be. Not only is it important that the actual lesion location fit into the treatment protocol selected by the ophthalmologist, but a misplaced laser irradiation site could cause severe vision loss. This implies the need to track any eye movements during irradiation and to adjust in real time the pointing of the laser to account for movement in such a way as to maintain the same lesion location. If eye movement exceeds the ability of the system to compensate, then the system must terminate laser irradiation.

Methods have been devised for eye tracking, but most are designed to monitor the anterior eye and cornea. To place lesions on the retinal surface with acceptable accuracy, the system must directly track the retina.[11] A few methods of tracking the retina directly have been devised.[11–14] For our purposes here, however, the choice of tracking methods is rather limited. When one accounts for the need to integrate (at reasonable cost) a photocoagulation laser control and pointing subsystem, an automatic lesion pattern generation subsystem, a lesion growth monitoring and control subsystem, *and* the retinal tracking subsystem of choice, with response times of 5 ms—and have it all work together seamlessly—then the most attractive tracking method is some combination of a global digital tracking technique and a high-speed analog technique. This choice is consistent with recommended algorithms for the rigid-body, translation-only tracking problem.[15]

3.1.1 *Conceptual design*

Initially, the feasibility of a robotic laser system for retinal surgery was studied.[6] The intent was to "develop an automated laser delivery system and retinal observation system that is capable of placing multiple lesions of predetermined sizes into known locations in the retina." Markow first demonstrated the concept of the system and identified key research objectives and technical hurdles required to make the system a reality. Over the course of several years and the work of many researchers (as discussed below), the optical design of the overall system evolved to that shown in Fig. 1. This design, including a digital tracker, an analog tracker, and a confocal reflectometer for lesion control is shown here to help orient the reader for the following discussion.

3.1.2 *Optical tracker*

Ghaffari investigated using an optical image correlation technique for retinal tracking.[16] In this technique, acousto-optical (A-O) cells performed the fine image matching operation. The cells "convert the real-time one-dimensional video information into a spatial light intensity controller system." Specifically, a two-dimensional template was generated to store a reference image. This image was then correlated to the real-time video frames. The result of this correlation was a new light distribution with a relative maximum located at the center of the best match. Retinal movement was calculated by measuring the movement of the relative correlation image maximum from one frame to the next. Ghaffari tested this system by tracking several different character symbols and simulated blood vessels. He reported a "±2.0% linearity in the horizontal and a ±1.8% linearity in the vertical directions. The tracking system can handle speed and acceleration of 656 degrees per second and 19,687 degrees per second^2 for 30 frames per second video rate. The accuracy of the tracking is within ±5 pixels in a 275 pixel square area." While the tracking speed was impressive, the susceptibility of correlation techniques to image noise and the difficulty of integrating this tracking method into the larger retinal surgery system led to more work on a digital approach to retinal tracking.

3.1.3 *Digital global tracker prototype*

Barrett et al. advanced the design of the digital retina tracker.[14] The digital tracking method uses a standard 30 frames per second (fps) charge coupled device (CCD) video camera attached to a nonmydriatic fundus camera to obtain an image of the retina for both tracking and the user interface. The CCD camera is connected to a frame grabber hosted by a standard desktop personal computer (PC). The digital tracking system provides a global retinal tracking capability using a blood vessel template to update the position of the irradiating laser on the retinal surface. Conceptually, a reference image (the tracking template) of the object to be tracked (the retina) is first obtained and a template is generated. When tracking is initiated, the tracking template is swept over incoming images of the object in real time. A match is found between the tracking template and the object image, and object movement information is derived from a change in the location of the template match. If no match can be found, a "loss of lock" signal is activated. Image changes can be categorized as translation, rotation, and/or scale. Translation is object displace-

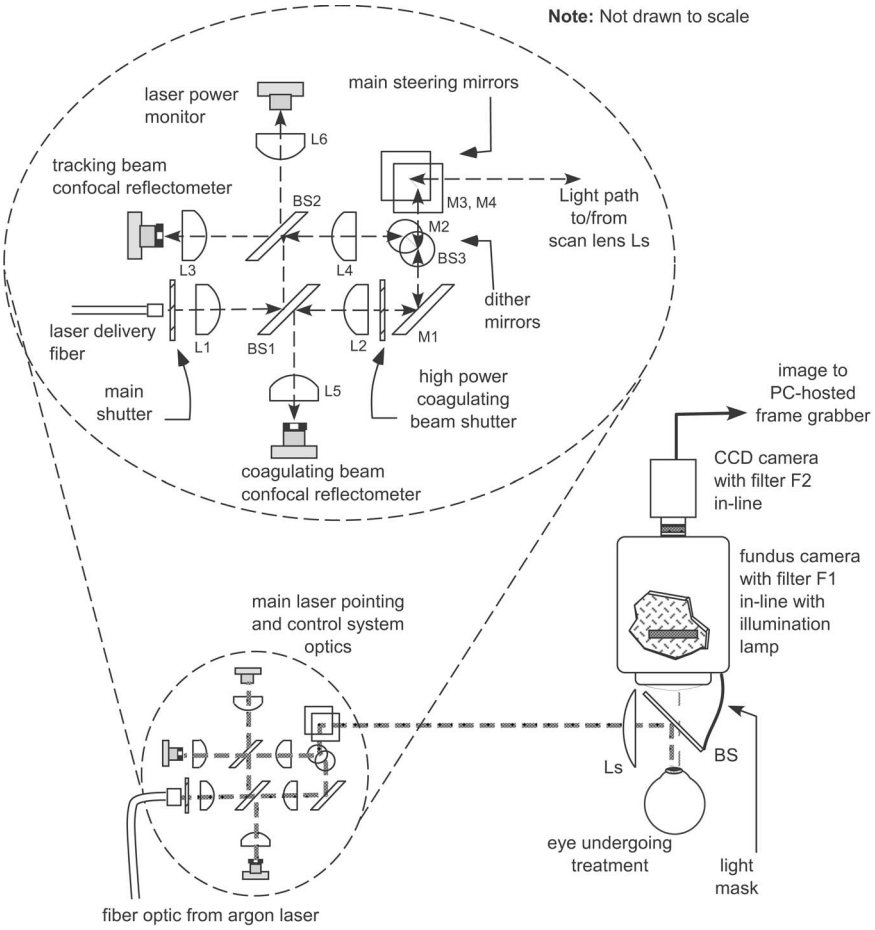

Fig. 1 Optical design of a computer-assisted laser retinal surgery system, including digital tracker, analog tracker, and confocal reflectometer for lesion control.

ment along the image abscissa, ordinate, or both. Rotation is an angular displacement around a specific axis. Scale is an object's increase or decrease relative to a fixed ratio within an image. The digital tracking method performs very well when compensating for translation. Rotation is not a significant problem, as noted by de Castro et al.: "… if small local deformations are neglected, during fixation the fundus apparently performs rigid plane movements, with small, if any rotational component."[17] Furthermore, because the distance between the camera image plane and the retina remains unchanged, scale changes are also minimal.

Template matching requires a reference image of the object. For this subsystem, we used six one-dimensional blood vessel templates to assemble a single two-dimensional retinal vessel "fingerprint" template. A pair of horizontal and vertical one-dimensional templates is selected from each third of a retinal area rich in vessels via the graphical user interface (GUI). The horizontal template chosen from the upper third of the reference image is designated as the first horizontal template. The other five one-dimensional template locations are referenced to the first horizontal template's location. This technique results in a computationally efficient model of the subject's retinal vessel pattern. See Fig. 2. With the template defined, the similarity metric to determine the "goodness" of the match between the template and the object image must be defined. There are a number of metrics for this, including maximum absolute error, mean absolute error, and mean-square error. For this design, we used the absolute value of the difference (AVD). The AVD method uses integer math to calculate the absolute value of the current template response minus the expected template response as a measure of match between the template and the object image. This similarity measure proved to be robust and computationally efficient.

There are several different methods of scanning the template over the object image. Ideally, one could calculate the template response at each and every pixel location within the object image, which is called an exhaustive search. While this would almost always yield a match on each object image, it is computationally expensive. For the retinal tracking subsystem, this would require calculating the AVD metric at approximately 60 000 pixel locations. The frame grabber providing the image data to the PC and a typical PC could not keep up with such a computational load while maintaining a lock on the retina. Another method is to use a coarse-fine technique. In this technique, the template is scanned over the image, regularly skipping over some fixed number of image rows and columns in a coarse search. Based on the template response from the coarse search, a fine (i.e., exhaustive) search is performed locally about the location of the coarse match to find the more exact match location. While this tech-

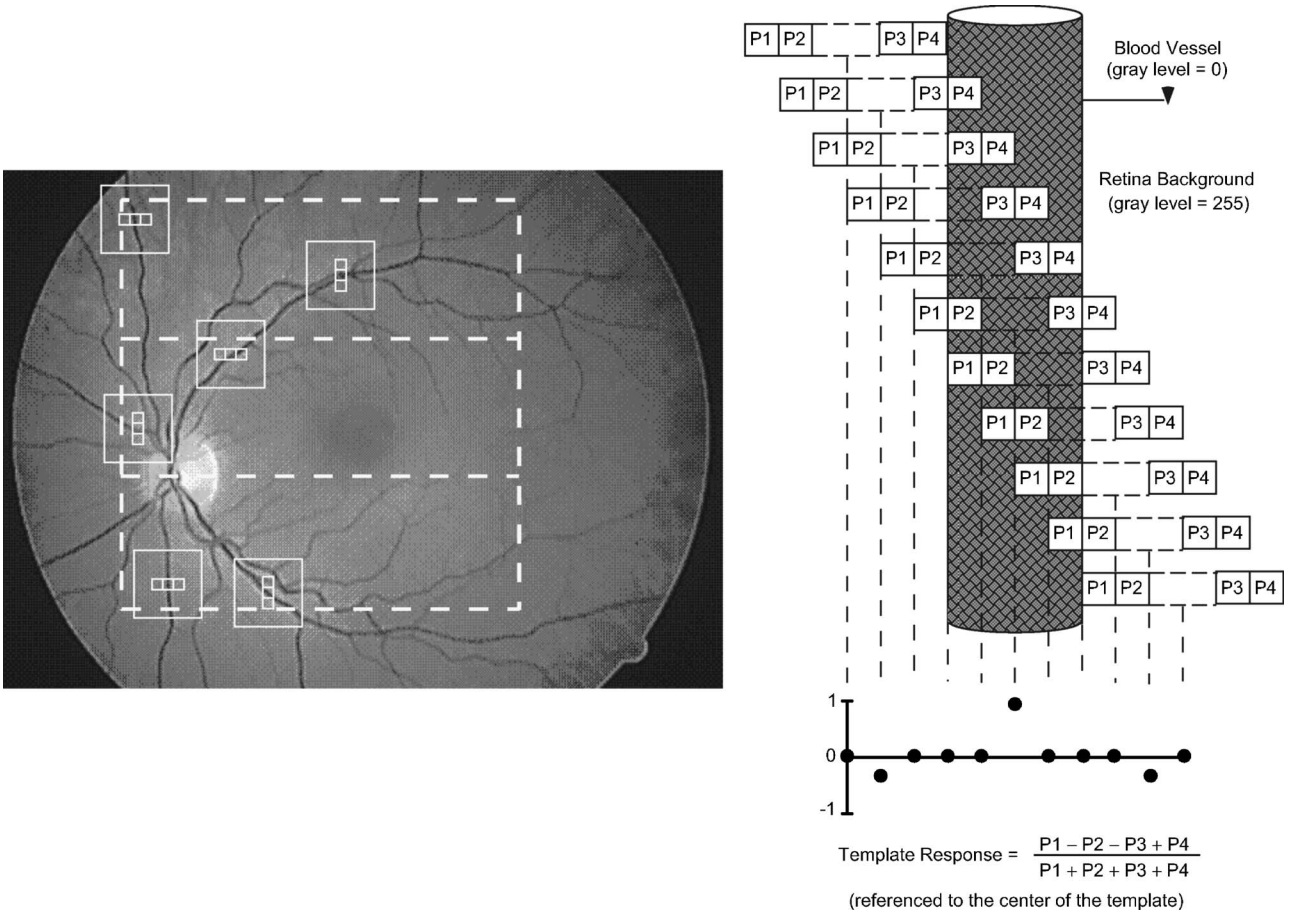

Fig. 2 The two-dimensional template used for the digital tracker. (a) Human fundus image with a two-dimensional template superimposed on the image. (b) Diagrammatic representation of a one-dimensional template response in the vicinity of a blood vessel.

nique speeds up the tracking task tremendously, there is a significant probability that the true match location may be skipped over during the coarse search. With this in mind, we used a limited-exhaustive search technique. In this technique, the object's velocity characteristics (i.e., the anticipated eye movements) are used to limit the search in subsequent frames to a small subregion of the image. For example, for a camera providing images at a standard rate of 30 fps, one can calculate how much the object could theoretically move during the 33 ms between frames. Because the location of the object is known in the present frame, we need only search a subregion of the subsequent frame centered about the last known match location. This technique tremendously speeds up the tracking task, yet avoids the danger of skipping over the true match location. However, should the tracked object move faster than anticipated, it will not be present within the subregion on the subsequent frame, and loss of tracking lock will occur.

While the digital tracker worked well, provided excellent integration into the overall system, and allowed the use of an intuitive GUI, its response time did not meet the specifications outlined earlier. While we could have moved to a faster frame rate camera, the higher cost, shorter integration time for the image, and increased data bandwidth would have created more problems than it solved. Thus we investigated a secondary, synergistic tracking method that would provide the necessary speed.

3.1.4 *Analog local tracker*

Wright and Ferguson worked together to integrate an analog tracking method into the system to complement the digital tracker.[18,19] The analog tracking subsystem locks onto a small area on the retina where the reflectance is significantly different than the surrounding tissue. Often a single laser-induced lesion is used for this, because the higher scattering coefficient of the denatured tissue makes it appear bright compared to the surrounding tissue in fundus images. We move a low-power secondary laser beam in a small circle ("dithering" the beam) around the designated reference lesion (often formed just for tracking purposes at the beginning of the procedure) and detect the returning light with a confocal reflectometer. At any given instant, when this "dithered" beam is pointed on the reference lesion, the reflectometer signal is high; when it is pointed off the lesion, the reflectometer signal is low. Thus the reflectometer output signal varies synchronously (when corrected for phase shifts) with the periodic dither signal which drives the pointing mirrors of the low-power secondary laser.

This output is processed to yield Δx and Δy error correction signals from the confocal reflectometer. The error signals initially increase as the center of the tracking beam's dither circle moves farther from the center of the reference lesion, and they contain all of the information needed to redirect the tracking beam back to the center of the reference lesion,

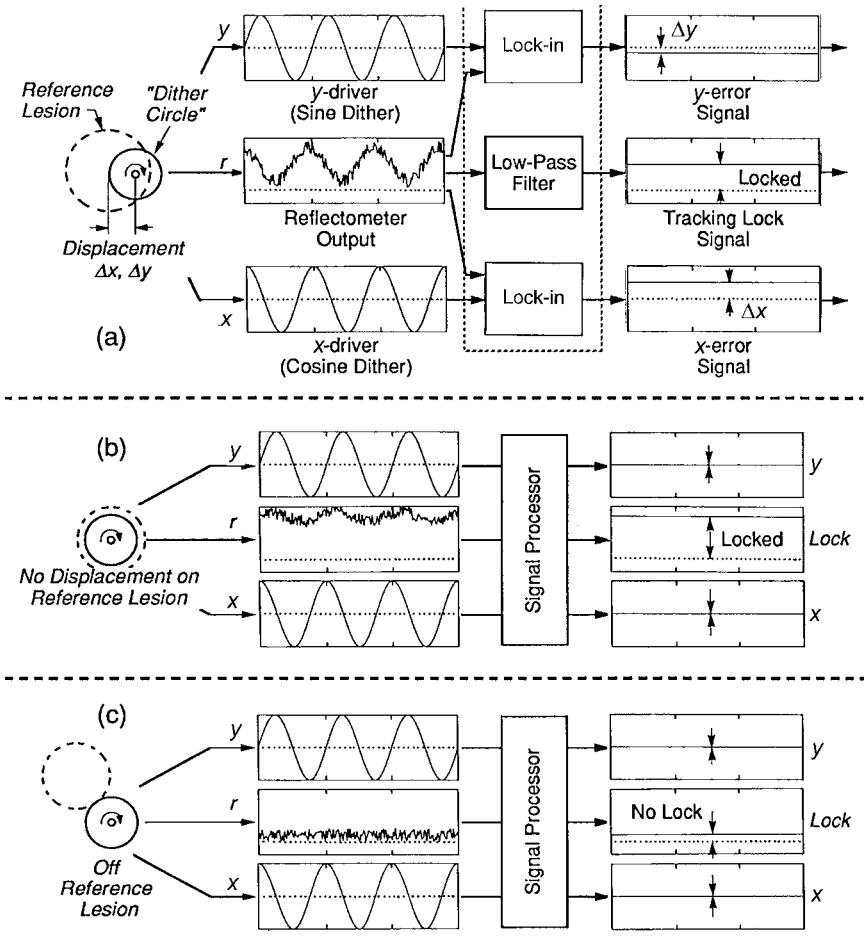

Fig. 3 Conceptual drawing of the analog tracking method. The *X* and *Y* sinusoidal signals sent to the dither beam pointing mirrors are in quadrature, resulting in a circular dither beam path. Phase-sensitive detection of the reflectance data returned from the dither beam, referenced to the phase of the *X* and *Y* sinusoidal steering signals, provides Δx and Δy error signals as shown in the diagram.

thereby minimizing the error signal, as illustrated in Fig. 3. By integrating these error signals over time, cumulative errors produce net displacements. Using these error signals to drive the main steering mirrors in the tracking beam path (which also directs the higher power coagulating beam), arbitrary motions of the reference lesion relative to the tracking beam can be followed. Because the reference lesion is fixed with respect to the retina, this results in retinal tracking. Such a control system is a variation on the servo loop concept.

Figures 3(a) to 3(c) depicts some representative dither circle signals and the resulting reflectometer signals. Phase-sensitive detection is accomplished with lock-in amplifiers,[20] which are simply analog multipliers (mixers) followed by low-pass filters, which produce dc offset voltages proportional to the amplitude component of the reflectometer signal which is in phase with the associated *X* or *Y* dither signal. The resulting pair of error voltages constitute a tracking correction vector that is relayed to the main steering mirrors. Note that in addition to the Δx and Δy error signals provided by the two lock-in amplifiers, a third signal is extracted from the reflectometer output: the average value of the returning light from the dither beam. Figure 3(a) shows a case in which the dither circle is displaced along the *x* axis (but not the *y* axis) relative to the reference lesion. There is a Δx error signal proportional to the displacement and a zero Δy error signal. Note the average value, or dc level, of the confocal reflectometer is significantly greater than zero. Figure 3(b) represents a case in which the dither circle is centered and locked on the reference lesion (the eye may or may not be stationary at this instant) so that null error signals are produced. Again the dc level of the confocal reflectometer is significantly greater than zero. In Fig. 3(c), the dither circle has "fallen off" the reference lesion completely and the error signals are meaningless. But note that the dc level of the confocal reflectometer signal is now very low. This low dc value condition allows such a loss of lock condition to be detected.

While this analog tracker is very fast and meets the response time requirements of the overall system, it is only a local tracker. That is, if the analog tracker "falls off" the reference lesion completely and loses lock, this subsystem has no way to reacquire the tracking lock on its own. However, the global tracking ability of the digital tracker can be brought into play to "help" the analog tracker reestablish the lock. This fact, plus the need for global fundus images used as part of the user interface, continue to make the digital tracker a necessary part of the overall system.

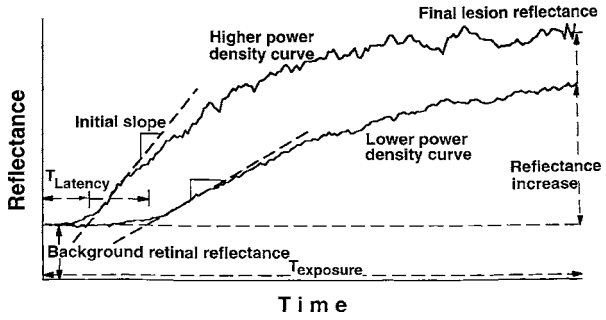

Fig. 4 Confocal reflectometry of lesion formation at two different laser power settings. The characteristic latency region, growing region, and saturation region is evident in both curves.

3.2 *Lesion Depth Control Subsystem*

As previously mentioned, current argon laser treatment protocols require the physician to preset the laser spot size, power, and irradiation time in hopes of achieving consistent therapeutic lesions across the surface of the retina. This is not a realistic expectation as the absorption properties across the retina are nonhomogeneous. In our investigations, we have seen the same laser parameters provide shallow lesions of nontherapeutic value, "good" therapeutic value lesions, anomalous lesions (with bubbles and other abnormalities), and retinal bleeding on the same retina.[21,22] This motivated Jerath et al. to develop the lesion depth control subsystem.[23,24] This subsystem's purpose is to dynamically control laser irradiation time during lesion formation to provide consistent lesions across the retinal surface.

The research goal for this subsystem has been to use visible, measurable lesion reflectance parameters as a noninvasive measure of lesion depth in real time. During therapeutic lesion formation, the reflective properties of the tissue change due to an increase in the tissue scattering coefficient.[25] This results in an increase in the amount of diffuse laser light reflected back from the lesion center.

Yang and Jerath used video images of the forming lesions to study lesion reflectance profiles.[21,23,26] Jerath was able to achieve consistent retinal lesions of prescribed depth or diameter using a UNIX-based workstation coupled to a fast frame CCD camera. The system was tested successfully on a model egg white medium and also *in vivo* on rabbit retinal tissue. Jerath demonstrated the capability to achieve reproducible, nearly identical lesions under conditions of varying absorption and laser power. The camera-based system was able to control lesion parameters in real time; however, the camera field of view required for lesion formation was not compatible with the camera field of view required for retinal tracking. Therefore, two separate cameras would be required using this technique.

To remedy this, Wright and Ferguson investigated the use of a confocal reflectometer to measure diffuse central reflectance of a lesion during laser irradiation. The basic premise behind confocal reflectometry is the use of a pinhole aperture to detect light only from the intended focal plane of interest and reject light from other regions. This allows for the isolation of the desired reflectance signal emanating from the central portion of the forming lesion. Therefore, specular reflection from the cornea or from other reflective surfaces within the system are effectively eliminated. Any reflection traveling along the central beam axis still passes through the pinhole aperture. However, the use of a small opaque beam block in the center of the lens eliminates this noise signal while having little effect on the diffuse reflected beam from the forming lesion.

The magnitude of the diffuse reflected light collected from the forming lesion using a confocal reflectometer has a characteristic, repeatable response, as shown in Fig. 4. The characteristic curve has three distinct regions: the latency region, the growing region, and the saturation region. The latency region is the period from when the retinal tissue is first illuminated with laser energy until the lesion starts to grow. The latency region is the flat part of the reflectance curve before the curve begins to rise. During this time interval, the retinal tissue absorbs laser light energy but does not achieve a temperature high enough for tissue coagulation. Once sufficient light energy is absorbed and coagulation occurs, the latency region ends and the lesion begins to grow quickly. This results in a corresponding steep rise in the reflectance signal called the growing region. Following this period of rapid growth, the

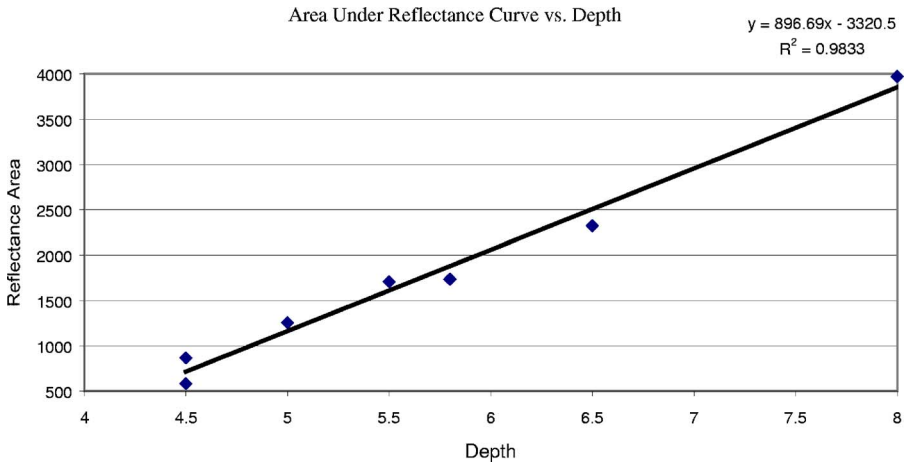

Fig. 5 Correlation between the area under the central reflectance curve of laser-induced lesions and the lesion depths.

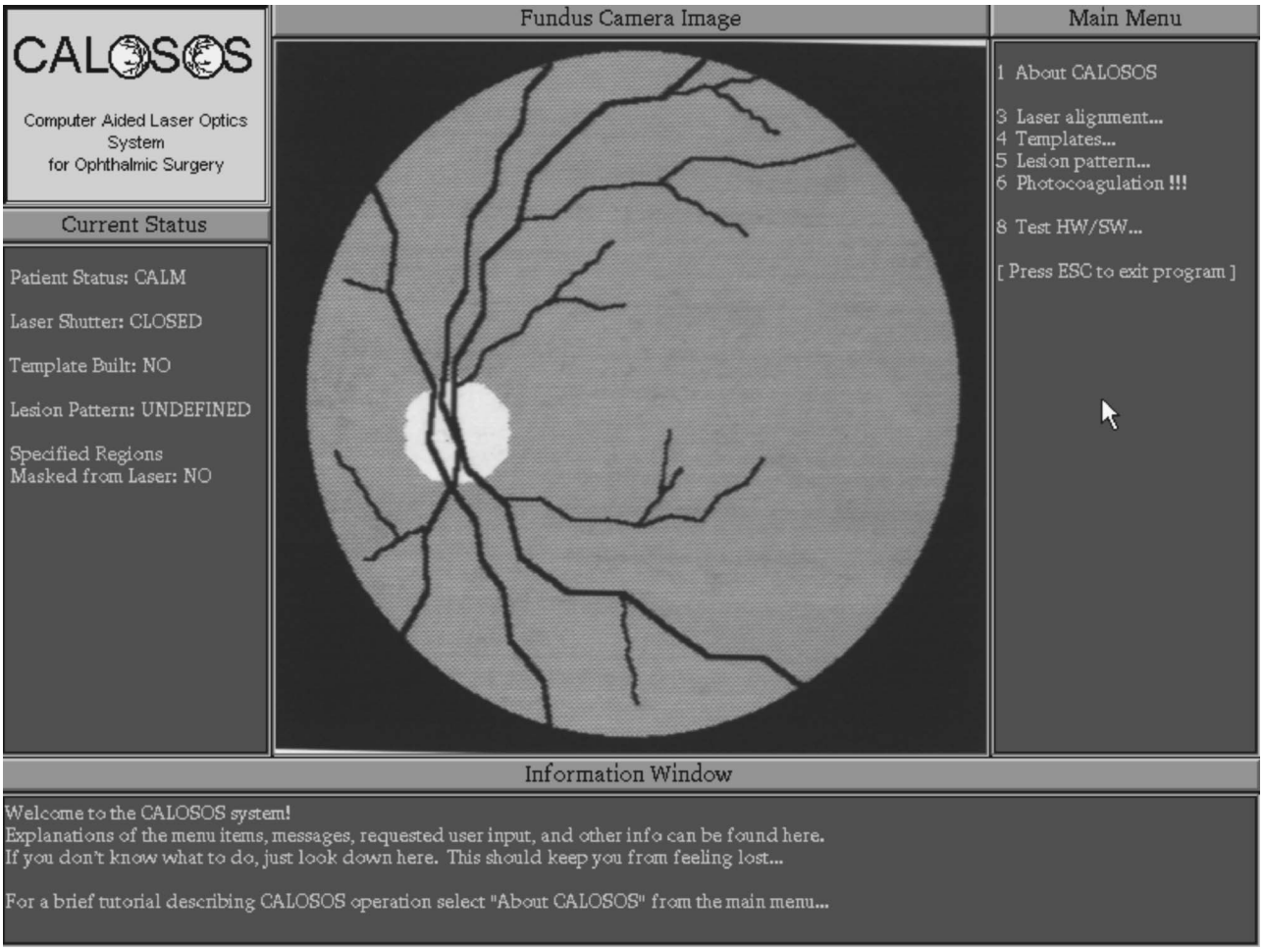

Fig. 6 Opening screen of the GUI. The left panel provides status information, the right panel provides menus for selecting various system actions, the bottom panel is used for messages to the user, and the center panel is a real-time video image of the retina provided by the fundus camera. A simulated retinal image is shown here.

reflectance curve flattens out into the saturation region. Should laser irradiation continue much beyond this point, overexposure will occur and result in significant retinal damage.

Barrett, de Graaf, and Wright attempted to correlate some measurable parameter of the lesion reflectance signal with the actual lesion depth. If a correlation could be found, the reflectance signal could then be used as a control signal for the laser shutter. They investigated the correlation between the latency period to lesion depth and the slope of the reflectance curve to lesion depth in a retinal phantom. Although these investigations yielded a promising (0.66 to 0.99) correlation coefficient between the visible lesion reflectance parameters and lesion depth, they did not believe the correlation was strong enough to be reliably used to control lesion depth parameters for laser surgery. They then investigated the correlation between the integrated lesion reflectance, the area under the lesion central reflectance curve, and lesion depth. Over the course of extensive experimentation using a variety of laser parameter combinations and purposely injected noise, they found that the correlation coefficient between the integrated central lesion reflectance and lesion depth varied between 0.90 and 0.99, as shown in Fig. 5.[27–31] Ludwig et al. and Naess et al. developed a microcontroller-based system to capture the reflectance signal from the confocal reflectometer and to produce a laser shutter control signal to develop lesions having consistent parameters.[32,33]

3.3 *User Interface*

One of the advantages the system provides, in addition to greater patient safety, is an easy to use, intuitive GUI developed by Wright. A representative GUI display is shown in Fig. 6.

Without any computer assistance, it is tedious for the ophthalmologist to manually identify all of the lesion locations required. For treatment of a condition such as diabetic retinopathy, this may be thousands of lesion sites. Each location must be chosen not only for its therapeutic value, but also to avoid critical areas such as the macula and major retinal blood vessels. The computer-assisted system incorporates a single-monitor, mouse-driven human/computer interface that helps the clinician designate the desired lesion locations and perform the surgical procedure.[19]

The reader may notice that Fig. 6 is not a Microsoft® Windows® interface. Due to the stringent real-time require-

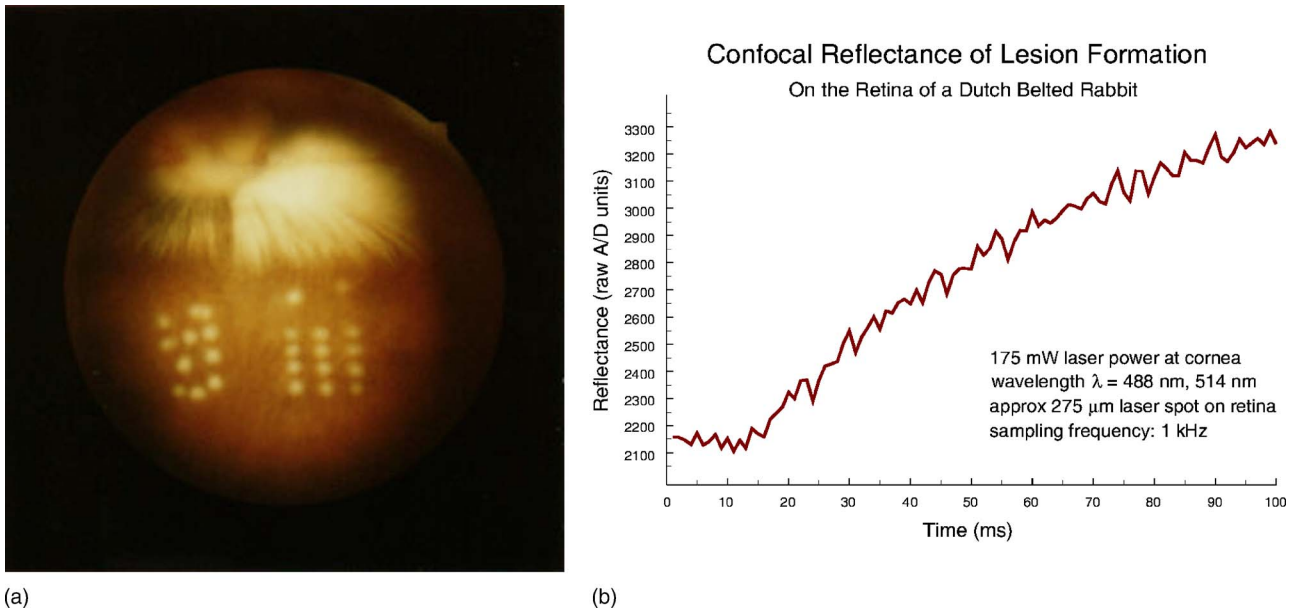

Fig. 7 Photocoagulation on a rabbit fundus, with unlocked and locked tracking, given eye motion of up to 32 deg/s. (a) Unretouched fundus image. (b) *In vivo* reflectance signal for a 100 ms irradiation on a rabbit fundus during motion-compensated tracking.

ments, low-level real-time operating system software was developed to control the system.

4 System Testing Results

The computer-assisted retinal laser surgery system was tested on stationary albumen eye phantoms, moving albumen eye phantoms, Dutch belted rabbits, and rhesus monkeys.

4.1 *Dutch Belted Rabbits*

An unretouched fundus image from one of the rabbits after testing is shown in Fig. 7(a). In this figure, the tracking lesion used for the analog tracker is the lesion closest to the center of the frame. Two 3×4 patterns of lesions were selected via the system GUI and created during eye motion of up to 32 deg/s. Each lesion is approximately 250 to 300 μm in diameter. The pattern on the left, intended to be rectangular, was created without correction signals from the analog tracker; it reveals the relative movement of the fundus during irradiation and shows why high-speed analog tracking is needed. The irregular lesion placement is due only to eye movement during the irradiation. The lesion pattern on the right was created with the analog tracker in the loop. This pattern shows the benefit of high-speed motion compensation, as well as the accuracy of the lesion pattern that can be created using the digital tracker's global coordinate system. The actual lesion locations in this pattern were no more than ±2 pixels (±64 μm on the retina) from the intended location specified via the system GUI.

In a frame-by-frame analysis of the fundus camera video tape of the entire experiment, the velocities of the rabbit's reflexive eye movements were determined. The maximum velocity the system could track without losing lock varied according to the optical condition of the cornea and the location of the reference lesion in the fundus field of view (FOV). A clearer cornea permitted faster velocities, as did a reference lesion near the center of the FOV. The lowest velocity at which tracking lock was broken was 30 deg/s during a short, highly impulsive movement. The highest velocity at which tracking lock was maintained was 38 deg/s, during a relatively smooth movement. A confocal reflectometer signal of a motion-stabilized lesion forming in 100 ms is shown on the right in Fig. 7(b).

4.2 *Rhesus Monkeys*

The Optical Radiation Branch of the Air Force Research Laboratory's Human Effectiveness Directorate is charged with performing minimum visible lesion (MVL) threshold studies for a variety of laser conditions. Some technologies, such as the ultrashort pulse laser, do not leave highly visible lesions. This complicates the postirradiation tissue analysis because the precise location of the lesion can be difficult to locate and thus analyze. To remedy this situation, laser professionals at the laboratory place visible row and column marker lesions with an argon laser. Ultrashort laser "lesions" are then placed at the cross section of the visible marker lesions. The visible lesions provide landmarks as an aid in locating the less visible ultrashort lesions in postexposure analysis. The MVL studies are typically accomplished *in vivo* on rabbits and rhesus monkeys, because the eyes of these species share many tissue properties with the human retina. Although the animal subjects are sedated during these procedures, retinal movement does occur, which complicates the placement of the lesion matrix field.

Barrett and Wright were invited by Optical Radiation Branch scientists to test the digital global tracker prototype system to see if it could be used to place the lesion matrices. An anesthetized primate subject was irradiated with both cw argon laser exposures of 150 mW at the cornea for 375 ms and single ultrashort pulses of up to 3 mJ at 120 fs. The cw laser wavelength was 514.5 nm and the ultrashort wavelength

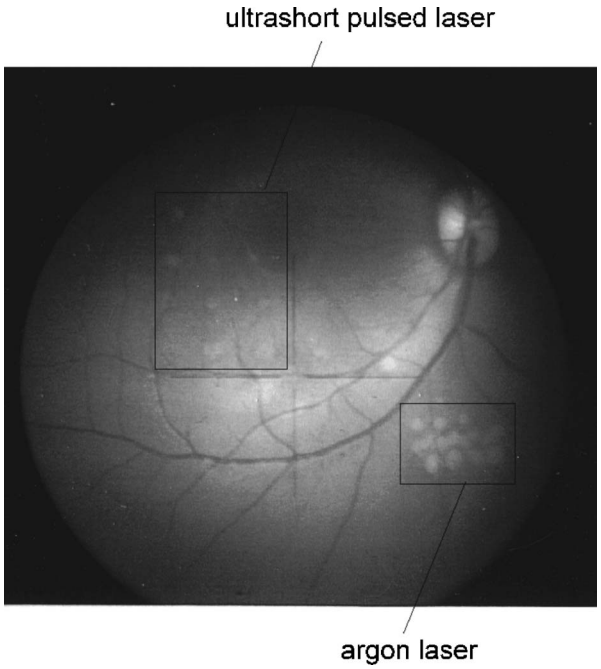

Fig. 8 Retinal image of a rhesus monkey after irradiation with both cw argon laser exposures of 150 mW at the cornea for 375 ms (lower right) and single ultrashort pulses of up to 3 mJ at 120 fs (upper left). The CW laser wavelength was 514.5 nm and the ultrashort wavelength was 580 nm.

was 580 nm (see Fig. 8). Although anesthetized, retinal movement occurred, allowing assessment of the power of the current methodology in precisely tracking the retina. Limited success was achieved due to difficulties in placing the optical system around the primate's abnormally large nose. Even so, the feasibility of using the system for lesion matrix placement in a primate subject was demonstrated.[34–36]

5 Follow-on Applications

A number of "spinoff" applications have made use of the technology developed for the computer-assisted retinal laser surgery system. For example, the system has been used to measure eye movement in retinal laser injury studies and has been adapted to track swimming rats in a Morris water maze. The system also shows promise for use in automated tattoo removal and mapping of dermal injury using a blue light laser. A brief description of each of these projects follow.

5.1 *Retinal Pathology Eye Movement Measurements*

Investigations demonstrate that ocular motility in eyes with retinal pathology may show a lower propensity to visit such areas of the retina as compared to nonpathological retinal sites. While current ophthalmic instruments with the ability to image both the retina and a visual function test target placed on the retina have provided this observation, the ability to quantify these images in real time as an eye movement measurement is presently lacking. We adapted the tracking algorithm described above to image the retina using a Rodenstock confocal scanning ophthalmoscope (CSLO) during the performance of a visual fixation task. Direct observation of acuity target placement at the retina under continuous viewing conditions was possible with this apparatus. Target fixation eye movement images of the retina were rapidly digitized from video tape records and registered using the retinal image tracking algorithm. Fixational eye movement pattern densities at the retina were derived from this data.

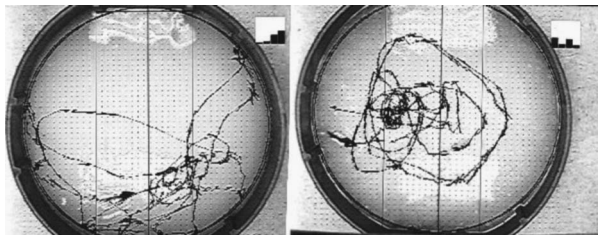

Fig. 9 Example tracking results for a rat swimming in a Morris water maze.

5.2 *Rat Tracking*

We adapted the tracking algorithm to track a rat swimming in a Morris water maze. The Morris water maze was developed by Professor Morris to measure memory retention in rodents. The water maze consists of a 2-m diameter pool filled with an opaque media such as water mixed with powdered milk or dispersed chalk. The opaque media prevents the rodent from obtaining visual cues on the location of a submerged platform. Hooded rats are used because the animals use visual cues to orient themselves, and their vision is more acute than albino rats. The dark fur on a rat's head provides a highly contrasted object for tracking against the white media, as shown in Fig. 9, allowing an update on rodent position 15 times per second. The tracking algorithm uses a rotation insensitive tracking template coupled with a limited exhaustive search technique to maintain lock on the moving rat. At the completion of the run, the relative time the rat spent in each quadrant was reported. The tracking algorithm was successfully used to evaluate the time course of memory loss and correlate that to tissue loss in the rat cortex following blunt trauma to the sensory cortex.

5.3 *Computer-Assisted Tattoo Removal*

Tattoos are made up of small, membrane enclosed ink granules held within perivascular dermal fibroblasts. Selective laser photothermolysis of tattoo ink is used to disrupt the ink granules without damage to adjacent dermal tissue, thus preventing subsequent scarring. If the skin is targeted by laser energy of a wavelength absorbed by the target ink granule over a brief period of time, the ink granule will be disrupted while cutaneous structures will dissipate the heat to their surroundings without injury. The Food and Drug Administration has approved the Q-switched neodymium:yttrium aluminum garnet (Nd:YAG) laser for tattoo removal. The laser is set for 10 pulses per second with a 3 to 4 mm spot size and an energy of 7 to 8 J/cm^2. Typical treatment time to remove a tattoo is four to eight 20 min sessions. We believe that the photocoagulation system described above would work well at automated tattoo removal, significantly reducing treatment time. That is, the template matching of the digital tracker could easily be set to follow the tattoo shape without tedious

human intervention. Any undesirable movement on the part of the patient would also be automatically compensated for by the system.

5.4 *Blue Light Dermal Imaging*

Ultraviolet light (200 to 400 nm, sometimes called "Wood's Light") has been used since 1903 to image skin disorders. More recently, Faraghan Medical Systems of Philadelphia has used a specialized Polaroid camera to photograph skin disorders with uv light. The uv light is more heavily absorbed in areas containing greater concentrations of melanin.

Overexposure to sunlight can damage the skin. After many years, this damage can cause skin cells to grow at an abnormally fast rate. The lesions formed when this occurs are called actinic keratoses (AK) and solaris keratoses (SK). The lesions formed have a higher concentration of melanin than the surrounding healthy skin. Therefore, when imaged with uv light, the lesions appear much darker than the surrounding skin. Over time, these lesions may grow and multiply forming large, unsightly areas on the skin. Not properly treated, they could lead to even more serious problems such as squamous cell carcinoma.

We are currently doing a preliminary study to use a computer-controlled blue light laser source (Liconix Helium Cadmium laser, 442 nm) to image skin diagnosed with both AK and SK. Melanin strongly absorbs blue wavelengths. Conceptually, a low-power laser will be scanned point-by-point (i.e., a raster scan) across the subject's face to produce a two-dimensional map of AK and SK locations. The highly adjustable laser pointing and tracking capabilities of the automated laser photocoagulation system is ideally suited to this task and can compensate in real time for patient movement while ensuring safety. The system could even start, stop, and restart the raster scan as needed without compromising the data by using facial landmarks recognized by the tracking system. The patient would then undergo treatment with flouruoracil as prescribed by the physician. The treatment success would be monitored with periodic AK and SK mappings. Using the automated system would greatly facilitate the detailed comparison of these mappings with one another to determine treatment progress.

6 Conclusions

Considerable design and development work occurred on the computer-assisted retinal laser surgery system at the University of Texas at Austin from the late 1980s through the mid-1990s. Welch continued to collaborate on the project with his former students Barrett and Wright, who were on the faculty at the U.S. Air Force Academy and the University of Wyoming. This later work focused on reducing the footprint of the laser delivery system optics and improving the lesion depth control subsystem. Other research groups have worked to improve the algorithms used to track the retina and to build retinal mosaic images using a Silicon Graphics workstation with interesting results.[37,38]

Originally, the primary challenge in developing a clinically significant yet affordable system was the lack of low-cost computer, camera, and frame grabber technology that could meet the necessary specifications. This is no longer the case. High-resolution, high-speed cameras with compatible frame grabbers are available from a number of manufacturers. Furthermore, computer speed and data transfer rates have significantly improved while prices have dropped. A fully capable computer-assisted retinal laser surgery system could be built today, based upon the proven design described in this paper, at very low cost and in a very compact case.

Acknowledgments

The authors extend their appreciation to H. Grady Rylander III, M.D., P.E., a fine engineer and practicing ophthalmologist whose collaboration on this project was essential. This work was supported by a number of research grants: the Texas Coordinating Board; the Office of Naval Research under Grant No. N00014-91-J-1564; the National Institutes of Health Grant No. 1R41EY10777; the Albert and Clemie Caster Foundation; the U.S. Air Force Office of Scientific Research; the Frank J. Seiler Research Laboratory at the USAF Academy, CO; Phillips Laboratory at Kirtland AFB, NM; and the University of Wyoming Office of Research and Economic Development.

References

1. J. M. Krauss and C. A. Puliafito, "Lasers in ophthalmology," *Lasers Surg. Med.* **17**(2), 102–159 (1995).
2. C. H. G. Wright, S. F. Barrett, and A. J. Welch, "Laser-tissue interaction," in *Medical Applications of Lasers*, D. R. Vij and K. Mahesh, Eds., Ch. 2, pp. 21–58, Kluwer Academic Publishers, Norwell, MA (2002).
3. S. F. Barrett, C. H. G. Wright, and A. J. Welch, "Laser ophthalmology," in *Medical Applications of Lasers*, D. R. Vij and K. Mahesh, Eds., Ch. 3, pp. 59–89, Kluwer Academic Publishers, Norwell, MA (2002).
4. G. L. Spaeth, Ed., *Ophthalmic Surgery: Principles and Practice*, W. B. Saunders, Philadelphia (1982).
5. R. Birngruber, V. P. Gabel, and F. Hillenkamp, "Fundusreflectometry: A step towards optimization of retina photocoagulation," *Mod. Probl. Ophthalmol.* **18**, 383–390 (1977).
6. M. S. Markow, A. J. Welch, H. G. Rylander III, and W. S. Weinberg, "An automated laser system for eye surgery," *IEEE Eng. Med. Biol. Mag.* **8**, 24–29 (1989).
7. D. G. Vaughan, T. Asbury, and P. Riordan-Eva, *General Ophthalmology*, 13th ed., Appleton and Lange Series, McGraw-Hill, New York (1992).
8. W. F. Ganong, *Review of Medical Physiology*, 16th ed., Appleton and Lange Series, McGraw-Hill, New York (1993).
9. E. J. Engelken, K. W. Stevens, W. J. McQueen, and J. D. Enderle, "Application of robust data processing methods to the analysis of eye movements," *Biomed. Sci. Instrum.* **32**, 7–11 (1996).
10. W. Kosnik, J. Fikre, and R. Sekuler, "Visual fixation stability in older adults," *Invest. Ophthalmol. Visual Sci.* **27**, 1720–1725 (1986).
11. D. P. Wornson, G. W. Hughes, and R. H. Webb, "Fundus tracking with the scanning laser ophthalmoscope," *Appl. Opt.* **26**, 1500–1504 (1987).
12. T. Bantel, D. Ott, and M. Rueff, "Global tracking of the ocular fundus pattern imaged by scanning laser ophthalmoscopy," *Int. J. Bio-Med. Comput.* **27**, 59–69 (1990).
13. M. S. Markow, H. G. Rylander III, and A. J. Welch, "Real-time algorithm for retinal tracking," *IEEE Trans. Biomed. Eng.* **40**, 1269–1281 (1993).
14. S. F. Barrett, M. R. Jerath, H. G. Rylander III, and A. J. Welch, "Digital tracking and control of retinal images," *Opt. Eng.* **33**, 150–159 (1994).
15. L. G. Brown, "A survey of image registration techniques," *ACM Comput. Surv.* **24**, 325–376 (1992).
16. S. Ghaffari, "The Design of a 2-Dimensional Optical Image Correlator and Its Application in Image Tracking," Ph.D. dissertation, University of Texas at Austin (1990).
17. E. de Castro, G. Cristini, A. Martelli, C. Morandi, and M. Vascotto, "Compensation of random eye motion in television ophthalmoscopy: Preliminary results," *IEEE Trans. Med. Imaging* **MI-6**, 74–81

(1987).
18. C. H. G. Wright, R. D. Ferguson, H. G. Rylander III, A. J. Welch, and S. F. Barrett, "Hybrid approach to retinal tracking and laser aiming for photocoagulation," *J. Biomed. Opt.* **2**, 195–203 (1997).
19. C. H. G. Wright, S. F. Barrett, R. D. Ferguson, H. G. Rylander III, and A. J. Welch, "Initial *in vivo* results of a hybrid retinal photocoagulation system," *J. Biomed. Opt.* **5**, 56–61 (2000).
20. M. L. Meade, *Lock-In Amplifiers: Principles and Applications*, Peregrinus Ltd, London (1983).
21. M. R. Jerath, D. Kaisig, H. G. Rylander III, and A. J. Welch, "Calibrated real-time control of lesion size based on reflectance images," *Appl. Opt.* **32**, 1200–1209 (1993).
22. C. H. G. Wright, J. K. Barton, D. E. Protsenko, H. G. Rylander III, and A. J. Welch, "Anomalous reflectance of laser-induced retinal lesions," *IEEE J. Sel. Top. Quantum Electron.* **2**, 1035–1040 (1996).
23. M. R. Jerath, R. Chundru, S. F. Barrett, H. G. Rylander III, and A. J. Welch, "Reflectance feedback control of photocoagulation in vivo," *Arch. Ophthalmol. (Chicago)* **111**, 531–534 (1993).
24. M. R. Jerath, R. Chundru, S. F. Barrett, H. G. Rylander III, and A. J. Welch, "Preliminary results on reflectance feedback control of photocoagulation in vivo," *IEEE Trans. Biomed. Eng.* **BME-41**, 201–203 (1994).
25. Y. Yang, A. J. Welch, and H. G. Rylander III, "Rate process parameters of albumen," *Lasers Surg. Med.* **11**, 188–190 (1991).
26. Y. Yang, M. S. Markow, H. G. Rylander III, W. S. Weinberg, and A. J. Welch, "Reflectance as an indirect measurement of the extent of laser-induced coagulation," *IEEE Trans. Biomed. Eng.* **37**, 466–473 (1990).
27. P. W. de Graaf, S. F. Barrett, and C. H. G. Wright, "A method to control irradiation time for laser photocoagulation of the retina," *Biomed. Sci. Instrum.* **34**, 82–86 (1998).
28. P. W. de Graaf, S. F. Barrett, and C. H. G. Wright, "A method to control irradiation time for laser photocoagulation of the retina: Part II," *Biomed. Sci. Instrum.* **35**, 159–163 (1999).
29. P. W. de Graaf, S. F. Barrett, and C. H. G. Wright, "Deriving irradiation control parameters for laser photocoagulation on the retina," *Biomed. Sci. Instrum.* **36**, 39–44 (2000).
30. C. H. G. Wright, S. F. Barrett, and P. W. de Graaf, "Determining laser dosimetry for consistent retinal photocoagulation," *Biomed. Sci. Instrum.* **37**, 197–202 (2001).
31. E. Naess, T. Molvik, S. F. Barrett, C. H. G. Wright, and P. W. de Graaf, "Irradiation control parameters for computer-assisted laser photocoagulation of the retina," in *Proc. SPIE* **4245**, 18–29 (2001).
32. D. A. Ludwig, S. F. Barrett, and R. F. Kubichek, "Laser dosimetry control for retinal surgery," *Biomed. Sci. Instrum.* **37**, 479–484 (2001).
33. E. Naess, T. Molvik, D. Ludwig, S. F. Barrett, S. Legowski, C. H. G. Wright, and P. W. de Graaf, "Computer-assisted laser photocoagulation of the retina: A hybrid tracking approach," *J. Biomed. Opt.* **7**, 1–11 (2002).
34. S. F. Barrett, C. H. G. Wright, E. D. Oberg, B. A. Rockwell, C. P. Cain, H. G. Rylander III, and A. J. Welch, "Digital imaging-based retinal photocoagulation system," in *Proc. SPIE* **2971**, 118–128 (1997).
35. B. A. Rockwell, D. X. Hammer, R. A. Hopkins, D. J. Payne, C. A. Toth, W. P. Roach, J. J. Druessel, P. K. Kennedy, R. E. Amnotte, B. Eilert, S. Phillips, G. D. Noojin, D. J. Stolarski, and C. P. Cain, "Ultrashort laser pulse bioeffects and safety," *J. Laser Appl.* **11**, 42–44 (1999).
36. S. F. Barrett, C. H. G. Wright, H. Zwick, M. Wilcox, B. A. Rockwell, and E. Naess, "Efficiently tracking a moving object in two-dimensional image space," *J. Electron. Imaging* **10**, 785–793 (2001).
37. D. E. Becker, A. Can, J. N. Turner, H. L. Tanenbaum, and B. Roysam, "Image processing algorithms for retinal montage synthesis, mapping and real-time location determination," *IEEE Trans. Biomed. Eng.* **45**, 105–118 (1998).
38. G. Lin, C. V. Stewart, B. Roysam, K. Fritzsche, G. Yang, and H. Tanenbaum, "Predictive scheduling algorithms for real-time feature extraction and spatial referencing: Application to retinal image sequences," *IEEE Trans. Biomed. Eng.* **51**, 115–125 (2004).